Electronic structure and physical properties of early transition metal mononitrides: Density-functional theory LDA, GGA, and screened-exchange LDA FLAPW calculations

C. Stampfl,[1] W. Mannstadt,[1,2] R. Asahi,[1,3] and A. J. Freeman[1]
[1]*Department of Physics and Astronomy, Northwestern University, Evanston, Illinois 60208-3112*
[2]*Fachbereich Physik, Philipps-Universität Marburg, 35032 Marburg, Germany*
[3]*Toyota Central R&D Laboratories, Inc., Nagakute, Aichi 480-1192, Japan*
(Received 23 October 2000; published 28 March 2001)

The desirable physical properties of hardness, high temperature stability, and conductivity make the early transition metal nitrides important materials for various technological applications. To learn more about the nature of these materials, first-principles density-functional theory calculations using the full-potential linearized augmented plane wave (FLAPW) method within the local-density approximation (LDA) and with the generalized gradient approximation (GGA) have been performed. We investigate the bulk electronic and physical properties of a series of early transition metal mononitrides, namely, those formed with 3*d* metals (ScN, TiN, VN), 4*d* metals (YN, ZrN, NbN), and 5*d* metals (LaN, HfN, TaN) in the rocksalt structure. In particular, lattice constants, bulk moduli, heats of formation, and cohesive energies as well as bulk band structures and densities of states are reported, and trends discussed. We find that the GGA yields 1%–2% larger lattice constants, 10%–20% smaller bulk moduli, and 10%–30% lower heats of formation compared to the LDA. The GGA slightly overestimates lattice constants, but leads *overall* to an improved agreement with experiment compared to the LDA, for which the values are too small. These materials are metallic with the exception of ScN, YN, and LaN, which appear to be semimetals within the LDA (and GGA), but are in fact *semiconductors* with indirect band gaps of 1.58, 0.85, and 0.75 eV, respectively, as revealed by calculations performed using the screened-exchange LDA approach. These last, relatively unexplored, refractory III-V nitrides may therefore have potential use in device applications; in particular, ScN is well lattice matched to GaN, a wide-band-gap semiconductor that is of great current interest in relation to optoelectronic devices, and high temperature and high power electronic applications.

DOI: 10.1103/PhysRevB.63.155106 PACS number(s): 71.20.Be

I. INTRODUCTION

The early transition metal (mono)nitrides, which crystallize in the rocksalt structure and are known as refractory compounds, exhibit extreme and unique physical properties of hardness, brittleness, high melting point, and in several of these compounds, a relatively high superconducting transition temperature [e.g., TiN and VN (Ref. 1), NbN (Refs. 2,3), and TaN (Ref. 4)]. Because of these properties, they have technological applications in the area of hard coatings[5] for cutting tools and potential uses as hard coatings for magnetic storage devices. In particular, the hardness of thin films of these materials can be significantly enhanced to ''superhardness'' (i.e., having a Vicker hardness of $\geqslant$40 GPa) by creating superlattices of nanoscale dimensions consisting of alternating layers, e.g., of TiN and VN.[6] And, very recently, a coating structure has been reported, nc-TiN/*a*-$TiSi_x$ (where nc denotes nanocrystalline and *a* amorphous), which reaches the hardness of diamond.[7] In order to understand the characteristic nature and behavior of these materials it is necessary, as a basis, to have a firm understanding of the bulk properties. In this respect, transition metal nitrides are also interesting from the point of view of fundamental studies due to their unusual and varied properties. In contrast to the transition metal oxides, they have received comparatively little attention.

There have been several earlier first-principles studies into the bulk properties of these materials: Papaconstantopoulos *et al.*[8] studied group V and VI transition metal mononitrides, focusing on superconducting properties, and MoN in particular. Zhukov *et al.*,[9] acknowledging that the transition metal nitrides (and carbides and oxides) usually contain vacancies, investigated TiN and VN (as well as their carbides and oxides) and the effect, in particular, that metalloid (N, C, or O) vacancies have on the bonding properties. Electronic, cohesive, and thermodynamic properties have been reported for 3*d* and 4*d* transition metal monocarbides and mononitrides in the rocksalt structure by Fernández Guillermet and Grimvall[10,11] and by Häglund *et al.*[12] Shimizu *et al.*[13] studied the electronic and magnetic properties of the mononitrides in the rocksalt and zinc sulfide structures formed with 3*d* transition metals. More recently, first-principles calculations on the magnetic properties of FeN (Refs. 14,15) and CrN (Ref. 16) have been reported. With respect to ScN, experiments have found it to be a semiconductor,[17–21] but also to be a compensated indirect semimetal.[22] Density-functional theory (DFT) calculations performed within the local-density approximation (LDA) find it is a semimetal.[23,24] It is well known, however, that the LDA underestimates the band gap of semiconductors.[25–27] Thus, there is some uncertainty at present concerning the electronic character of ScN and it is desirable therefore to use a theoretical approach that describes the band gap more accurately in order to investigate the electronic structure of this material and to establish its nature.

In this paper, we report first-principles all-electron density-functional full-potential linearized augmented plane

wave (FLAPW) calculations for a series of *early* (nonmagnetic) transition metal mononitrides, namely, those formed with 3*d* metals (ScN, TiN, VN), with 4*d* metals (YN, ZrN, NbN), and with 5*d* metals (LaN, HfN, TaN)—all in the rock-salt structure. We are interested in the bulk properties of these materials and in particular report the electronic structure, lattice constants, and bulk moduli, as well as the heats of formation and cohesive energies. We employ the LDA and generalized gradient approximation (GGA) for the exchange-correlation functional and investigate any improvements brought about by the GGA. Recent overviews concerning the performance of GGA's can be found in Refs. 28 and 29. Indeed, for many molecules and solids GGA's have been shown to yield more accurate binding (or cohesive) energies than the LDA. Reaction and activation energies for various chemical reactions as well as for the adsorption of adparticles on surfaces of metals and semiconductors are likewise improved (see, e.g., Ref. 30 and 31 and references therein). While GGA's tend to yield larger crystal equilibrium volumes compared to the LDA, they do not *in general* lead to more accurate structural or elastic parameters than the LDA compared to experiment, and some limitations have been pointed out.[32–34] However, the relative *energetic stability* of some structural phases has been reported to be better described for magnetic and nonmagnetic systems.

In contrast, band gaps for the III-V nitrides (AlN, GaN, and InN) were found not to be improved with the GGA,[35] although there have been conflicting results for transition metal oxides in the literature: studies by Dufek *et al.*[36,37] reported a significant improvement in the band structure when using the GGA: in an earlier publication, however, Leung *et al.*[38] reported no significant change in the band structure between LDA and GGA results for the same materials.

Hence, for ScN (and YN and LaN), which are the most likely candidates to exhibit semiconducting behavior due to the complete filling of bonding states and completely unoccupied non-bonding and antibonding states,[22] we have calculated band structures using the GGA—and have also investigated the excited state properties using the screened-exchange (sX) LDA.[39–42] Such an approach is less computationally demanding than the *GW* method[43] and also permits self-consistent determination of electronic structures as well as eigenfunctions.[41] It has also been shown to yield better agreement than the LDA with experimental values for lattice constants and band gaps.[39–41].

II. CALCULATION METHODOLOGY

The density-functional theory calculations are performed using the first-principles FLAPW method[44] with the local-density approximation[45] as well as the generalized gradient approximation[46] for the exchange-correlation functional. Selected calculations are also performed using the recently implemented[41] sX-LDA for ScN (and YN and LaN) for which there is some question as to the nature of the excited state band structure. Angular momenta up to $l_{max}=8$ in the muffin-tin spheres for both the wave functions and charge density are used in the self-consistent cycles. The muffin-tin radii R_{MT}, **k**-point set, and plane-wave cutoffs $K_{\max}$ for each transition metal nitride system were carefully tested. Those used are listed in Table I along with the calculated bulk physical properties, namely, the lattice constants, bulk moduli, and heats of formation. The heats of formation are obtained by considering the reaction to form (or decompose) crystalline bulk nitrides from (or into) the elements:

$$X(\mathrm{solid})+\frac{1}{2}\mathrm{N}_2(\mathrm{gas})\rightleftharpoons X\mathrm{N}(\mathrm{solid}),$$

where X stands for the metal atom. Then from the respective total energies of these phases we obtain the heat of formation as

$$\Delta H_f^0=(E_{\mathrm{tot}}^X+1/2E_{\mathrm{tot}}^{\mathrm{N}_2})-E_{\mathrm{tot}}^{X\mathrm{N}}, \tag{1}$$

where $E_{\mathrm{tot}}^{X\mathrm{N}}$, $E_{\mathrm{tot}}^{\mathrm{N}_2}$, and E_{tot}^X are, respectively, the total energies of the bulk nitride system, the free N_2 molecule, and the bulk metal. (Here we have defined a positive value to represent an exothermic reaction and a negative value an endothermic one.)

In obtaining the required bulk metal total energy (the corresponding atomic structure for the metal series studied is either hexagonal close packed or body-centered cubic), we optimized the crystal volume to be consistent with the rest of our calculations in which the structures are also optimized to their theoretical equilibrium geometries. (For the hexagonal structures, the c/a ratio was fixed at the experimental value and the lattice constant a was varied to optimize the volume.) We found that the metal lattice constants were between 1.5% and 3.0% smaller than the experimental values for the LDA; the values obtained using the GGA were 2.2%–3.3% larger than those of the LDA and thus very close to experiment (to within -1.2%–0.0%).

With respect to the N_2 molecule, we placed the molecule in a cube with side length of up to 14 Bohr and used the $(\frac{1}{4}\frac{1}{4}\frac{1}{4})$ **k** point for the Brillouin zone integration, which yields faster convergence than the Γ point. The bond length was calculated to be 1.09 Å within the LDA and 1.10 Å within the GGA, in good agreement with other calculations e.g., 1.099 (Ref. 35) and 1.085 (Ref. 47) for the LDA and 1.105 (Ref. 35), 1.095 (Ref. 47) for the GGA, as calculated using DFT with the pseudopotential method, and 1.1095 (Ref. 47) and 1.102 (Rev. 47) for the LDA and the GGA, respectively, as calculated using the full-potential linearized augmented plane wave method. The experimental value is 1.098 Å.[48]

Since use of the sX-LDA method is relatively recent we outline it briefly. The method was first proposed by Bylander and Kleinman[39] in order to obtain a more accurate description of the band gap. Seidl *et al.*[40] showed that the method can be introduced as a particular case of the generalized Kohn-Sham (KS) framework, the essence being that the energy functional can include some part of the *interacting* energy functional as well as the noninteracting one (as employed in the KS scheme). The single-particle equation is then written as

TABLE I. Lattice constant a_0, bulk modulus B, and heat of formation ΔH_f^0 for a series of early transition metal mononitrides in the rocksalt structure. Also listed are the plane wave cutoffs $K_{\max}$ and muffin-tin radii R_{MT}. The calculational parameters employed are the same for the GGA as for the LDA except where explicitly indicated. The number of **k** points used in the irreducible part of the Brillouin zone is 60 in all cases [the folding parameters for the Monkhorst-Pack scheme (Ref. 56) are (8 8 8)].

System	Method	a_0 (Å)	B (Mbar)	ΔH_f^0 (eV)	$K_{\max}$	R_{MT} (bohr)
ScN	Present FLAPW-GGA	4.50	2.01	4.32		$R_{\mathrm{Sc}}=2.55,\ R_{\mathrm{N}}=1.5$
	Present FLAPW	4.42	2.35	4.80	4.3	$R_{\mathrm{Sc}}=2.4,\ R_{\mathrm{N}}=1.7$
	LAPW [a]	4.54	2.18			
	Expt.	4.50 [b],4.44 [c]				
TiN	Present FLAPW-GGA	4.26	2.86	3.56		
	Present FLAPW	4.18	3.22	4.36	5.3	$R_{\mathrm{Ti}}=2.4,\ R_{\mathrm{N}}=1.4$
	LAPW [a]	4.24	3.05			
	LMTO-ASA [d]	4.32	3.89			
	Expt.	4.24 [e], 4.242 [f], 4.235 [c]	2.88 [d]			
VN	Present FLAPW-GGA	4.12	3.33	2.00		
	Present FLAPW	4.06	3.76	2.78	5.8	$R_{\mathrm{V}}=2.2,\ R_{\mathrm{N}}=1.4$
	LAPW [a]	4.07	4.14			
	APW [g]	4.14				
	LMTO-ASA [d]	4.23	2.82			
	Expt.	4.14 [h], 4.141 [f]	2.33 [d]			
YN	Present FLAPW-GGA	4.85	1.63	3.78		
	Present FLAPW	4.77	2.04	4.33	4.05	$R_{\mathrm{Y}}=2.9,\ R_{\mathrm{N}}=1.5$
	Expt.	4.877 [i]				
ZrN	Present FLAPW-GGA	4.57	2.64	3.82		
	Present FLAPW	4.53	2.92	4.48	4.3	$R_{\mathrm{Zr}}=2.6,\ r_{\mathrm{N}}=1.5$
	Expt.	4.537 [f], 4.61 [c]				
NbN	Present FLAPW-GGA	4.42	3.17	1.93		
	Present FLAPW	4.36	3.54	2.65	4.05	$R_{\mathrm{Nb}}=2.6,\ R_{\mathrm{N}}=1.5$
	APW [g]	4.38				
	Expt.	4.392 [f]				
LaN	Present FLAPW-GGA	5.32	1.48			
	Present FLAPW	5.27	1.73	3.20	4.05	$R_{\mathrm{La}}=2.7,\ R_{\mathrm{N}}=1.8$
	Expt.	5.295 [f], 5.301 [c]				
HfN	Present FLAPW-GGA	4.54	2.78			
	Present FLAPW	4.48	3.20	4.13	4.05	$R_{\mathrm{Hf}}=2.6,\ R_{\mathrm{N}}=1.5$
	Expt.	4.52 [f]				
TaN	Present FLAPW-GGA	4.42	3.38	1.70		
	Present FLAPW	4.37	3.78	2.48	4.05	$R_{\mathrm{Ta}}=2.5,\ R_{\mathrm{N}}=1.5$
	APW [g]	4.40				
	Expt.	4.385 [f]				

[a]Reference 13.
[b]References 57–60.
[c]Reference 61.
[d]Reference 9.
[e]Reference 62.
[f]Reference 63.
[g]Reference 8.
[h]Reference 64.
[i]Reference 65.

$$\left[\frac{-\hbar^2}{2m}\nabla^2+v_{eff}(\mathbf{r})\right]\psi_i(\mathbf{r})+\int d\mathbf{r}'v_{sx}^{NL}(\mathbf{r},\mathbf{r}')\psi_i(\mathbf{r}') - v_{sx}^{L}(\mathbf{r})\psi_i(\mathbf{r})=\varepsilon_i^{sx}\psi_i(\mathbf{r}), \tag{2}$$

where $v_{eff}(\mathbf{r})$ is the effective potential from the LDA and v_{sx}^{NL} and v_{sx}^{L} are nonlocal and local screened-exchange potentials. From Eq. (2) it follows that

$$E_g^{sx}=\varepsilon_{N+1}^{sx}[n]-\varepsilon_N^{sx}[n] =\varepsilon_{N+1}^{LDA}[n]-\varepsilon_N^{LDA}[n]+\langle\psi_{N+1}|\hat{v}_{sx}^{NL}-\hat{v}_{sx}^{L}|\psi_{N+1}\rangle -\langle\psi_N|\hat{v}_{sx}^{NL}-\hat{v}_{sx}^{L}|\psi_N\rangle, \tag{3}$$

where E_g^{sx} is the energy band gap obtained from the sX-LDA method. We note that this self-consistent approach has been

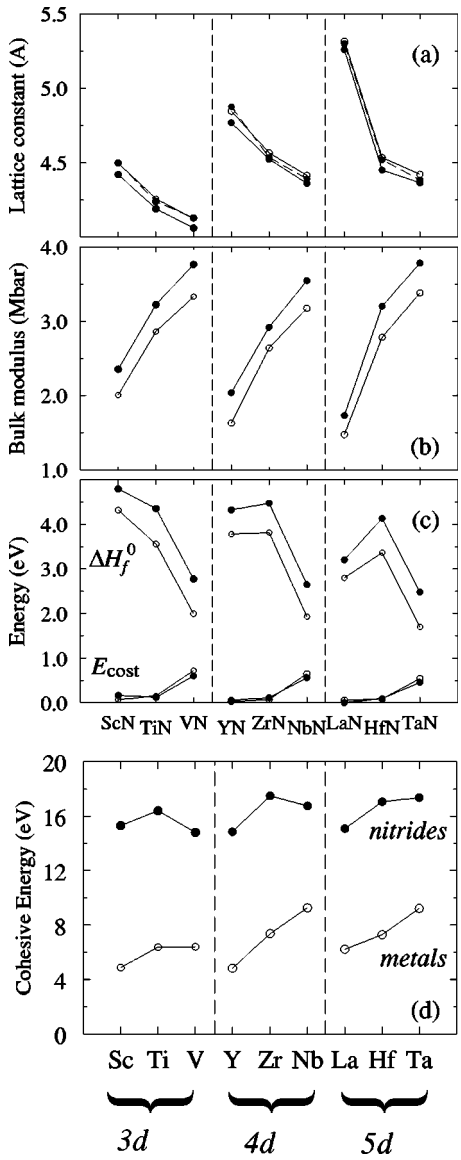

FIG. 1. (a) lattice constants, (b) bulk moduli, and (c) heats of formation ΔH_f^0 (upper curves) and energy cost [see Eq. (4)] for bulk metal distortion, $E_{\rm cost}$ (lower curves). Results obtained using the LDA and the GGA are represented by the full and open circles connected by a continuous line, respectively. Experimental results for the lattice constants are denoted by full circles connected by a dashed line. (d) Cohesive energies of the nitrides (upper curves and full circles) and of the bulk metals (lower curves and open circles).

formulated and implemented, not just for bulk calculations,[41] but also for superlattices and film geometries where the linear response is spatially nonuniform.[42]

III. RESULTS

A. Physical properties

The calculated lattice constants, bulk moduli, and heats of formation are listed in Table I, as obtained using the LDA and the GGA. Where possible, we have included the results of other *ab initio* calculations and experimental values. Our calculated results are also presented in Fig. 1 where the trends can be seen more easily. On going from ScN to TiN to VN (left to right in the periodic table with respect to the metal atom), where the metal 3*d* states are being consecutively filled, i.e., having one, two, and three electrons, respectively, it can be seen that the lattice constant decreases [Fig. 1(a)] and the bulk modulus increases [Fig. 1(b)]. A similar trend is seen for the 4*d* metal and 5*d* metal nitride materials. Such a trend is also observed for the bulk metals, which is explained in terms of the filling of the *d* bands.[49] On going down the columns of the periodic table, the lattice constant exhibits an increase in accordance with the larger size of the metal atom. The results obtained using the LDA and the GGA show the same trends, with the GGA yielding 1%–2% larger lattice constants and 10%–20% smaller bulk moduli compared to the LDA. The GGA yields closer agreement with experiment, although the lattice constant is slightly overestimated.

The heat of formation [Fig. 1(c)] calculated using the LDA exhibits a decrease for the 3*d* metal nitrides on going from left to right in the periodic table. For the 4*d* and 5*d* series a small (0.15 eV) and larger (0.93 eV) increase is initially observed on going from YN to ZrN and from LaN to HfN, respectively. This is followed by a strong decrease, as for the 3*d* series, of 1.6 eV on going from ZrN to NbN and of 1.9 eV on going from HfN to TaN. The heats of formation calculated within the GGA exhibit the same trend as in the LDA but are from 10% to 30% smaller. We note that a similar behavior with respect to the GGA relative to the LDA has been reported for the III-V nitrides (AlN, GaN, and InN).[35,47] The trend of a sharp decrease on going from TiN to VN is also found in Ref. 10 using a generalized approach that combines theory and experiment, and for YN, ZrN, and NbN, the work of Ref. 50, which uses the augmented spherical wave method, finds a similar trend to what is found here. This trend is also reproduced by a semiempirical method;[51] the trend in the study of Guillermet *et al.*[11] differed in that a higher heat of formation was found for YN as compared to ZrN.

With respect to the significant decrease in the heat of formation observed for VN, NbN, and TaN, part of the reason for this can be related to the metal-metal bonds of the material, in that in the nitride compounds they are considerably stretched compared to their bulk values, namely, by 12.9%, 10.4%, and 7.7% (LDA) and by 12.8%, 9.2%, and 8.4% (GGA), for V, Nb, and Ta, respectively. For the nitrides to the left of these, i.e., all the others nitrides considered here, the difference in the bond length of the metal in the bulk phase and at the atomic positions it has in the nitride compound, is notably smaller, i.e. only between -3.4% and 4.4% (LDA) and -3.6% and 4.5% (GGA), and thus so is the associated energy cost to change the metal-metal bond length. Furthermore, on going from left to right in the periodic table, for the metals considered here, the energy cost for distortion of the metal bonds has been shown to increase, as discussed by Gelatt *et al.*[50] This energy cost $E_{\rm cost}$ is also shown in Fig. 1(c) (lower curves) together with the heat of formation. It is obtained as

$$E_{\rm cost} = E_{\rm tot}^{\text{metal fcc}(XN)} - E_{\rm tot}^{X}, \tag{4}$$

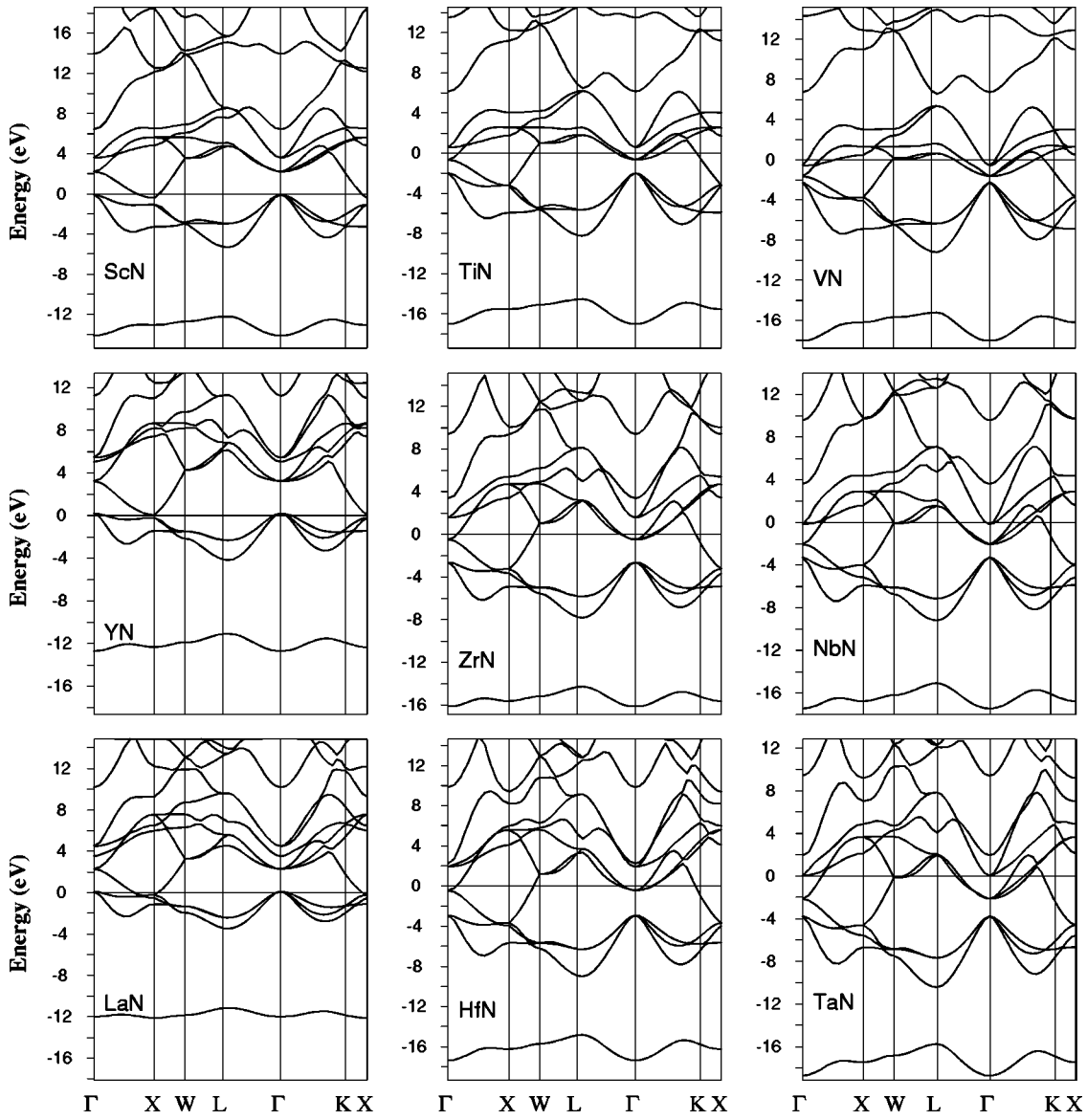

FIG. 2. LDA bulk band structures for the early transition metal nitrides studied in the rocksalt structure arranged corresponding to the position of the metal atom in the periodic table.

where E_{tot}^{X} and $E_{\mathrm{tot}}^{\mathrm{metal\ fcc}(X\mathrm{N})}$ are the total energies per atom of the bulk equilibrium structure of the transition metal and of the transition metal in the fcc structure at the lattice constant of its mononitride, respectively.

On first consideration, values of the heat of formation that do not monotonically increase from left to right in the periodic table may seem counter-intuitive in relation to their lattice constants, which *decrease* from left to right, and the corresponding bulk moduli, which *increase* from left to right. That is, it could be expected that for materials with have a smaller lattice constant and larger bulk modulus, the bond strength would be stronger and the cohesive energy larger, and consequently the heat of formation also larger. In order to understand the values of the heat of formation, we express it as

$$\Delta H_f^0 = E_{\mathrm{coh}}^{X\mathrm{N}} - E_{\mathrm{coh}}^{X} - 1/2E_{\mathrm{bind}}^{\mathrm{N}_2}, \tag{5}$$

where $E_{\mathrm{coh}}^{X\mathrm{N}}$ and E_{coh}^{X}, are the cohesive energies of the nitride compound and the metal, respectively, and $E_{\mathrm{bind}}^{\mathrm{N}_2}$ is the binding energy of the N_2 dimer. While the last value obviously remains the same for all the compounds, the cohesive energy of the metal varies across the periodic table; in particular, it generally peaks in the middle of the transition metal series (i.e., from row IIIB to IB in the periodic table).[49] Thus, the trend in the heat of formation of the nitrides will be a result of the relative changes in the cohesive energies of the nitride compounds and the bulk metals across the series. The cohesive energies of the nitride compounds and the bulk metals, as calculated using the LDA, are shown in Fig. 1(d).

For the total energies of the free atoms required in the calculation of cohesive energies in Fig. 1(d) we use the LAPW-calculated values of Ref. 52. The bulk metal cohesive energy is given by $E_{\mathrm{coh}}^{X} = E_{\mathrm{tot}}^{\mathrm{free}X} - E_{\mathrm{tot}}^{X}$, where $E_{\mathrm{tot}}^{\mathrm{free}X}$ is the total energy of the free metal atom, and the cohesive

TABLE II. Characteristic energy gaps of the band structures shown in Fig. 2. (See text for an explanation of the various energy gaps.) For ScN, YN, and LaN, the values in brackets are those obtained using the sX-LDA approach.

Energy gaps (eV)	ScN	TiN	VN
$E_{\mathrm{Ns-N}p}$	6.94 (9.10)	6.38	5.25
ΔE_d	2.30 (4.70)	1.29	0.58
$E_p - E_s$	14.07 (15.88)	15.05	15.80
$E_g^{\Gamma_{15}-X_5}$	(1.58)		
$E_g^{X_3-X_5}$	(2.41)		
	YN	ZrN	NbN
$E_{\mathrm{Ns-N}p}$	7.46 (8.94)	6.57	6.01
ΔE_d	3.03 (4.52)	2.11	1.24
$E_p - E_s$	13.06 (15.88)	13.50	14.18
$E_g^{\Gamma_{15}-X_5}$	(0.85)		
$E_g^{X_3-X_5}$	(1.15)		
	LaN	HfN	TaN
$E_{\mathrm{Ns-N}p}$	7.78 (10.34)	5.96	5.44
ΔE_d	2.19 (3.93)	2.46	1.61
$E_p - E_s$	12.11 (14.22)	14.45	14.96
$E_g^{\Gamma_{15}-X_5}$	(0.75)		
$E_g^{X_3-X_5}$	(1.01)		

energy of the nitride is given by $E_{\mathrm{coh}}^{XN} = -E_{\mathrm{tot}}^{XN} + E_{\mathrm{tot}}^{\mathrm{free}X} + E_{\mathrm{tot}}^{\mathrm{free\ N}}$), where $E_{\mathrm{tot}}^{\mathrm{free\ N}}$ is the total energy of the N atom (again defining a positive value as representing a bound system).

Considering first the 3*d* nitride series, the drop in ΔH_f^0 on going from ScN to TiN can be seen from Fig. 1(d) to be due to the fact that the increase in the metal cohesive energy is greater than that of the nitride [cf. Eq. (5)], and on going from TiN to VN, even though the metal cohesive energy does not change very much, that of VN is considerably less than that of TiN. For the 4*d* series on going from YN to ZrN, the cohesive energy of ZrN also increases as does that of the metal Y; in this case, the increase in the nitride is slightly greater than that of the metal so we observe a slight increase in ΔH_f^0. The significant decrease from ZrN to NbN is a consequence of the fact that the cohesive energy of NbN is less than that of ZrN, *and* the cohesive energy of Nb is greater than that of Zr [see Fig. 1(d) and Eq. (5)]. Similar considerations can explain the heats of formation for the 5*d* series.

Thus, we see in fact that the cohesive energies of the nitrides do exhibit a similar trend to their constitutent metals for the first two columns: an increase in the bulk modulus, a decrease in the lattice constant, and an increase in the cohesive energy. And in these nitrides, the metal-metal distance is similar to that in the bulk metal. It is only for the third column nitrides (for VN, NbN, and TaN) that there is a deviation; in particular, the cohesive energy does not increase (VN and NbN) from left to right (i.e., from second to third column), or it increases much less (TaN) than in the case for the change from first to second column, which results in a noticeable drop in ΔH_f^0. We attribute this behavior to the fact that the metal-metal distance in the nitride compounds in this third column is significantly larger than in the bulk metal and so the system does not gain this metal-metal bonding—in contrast to the nitrides in the first and second column. This could be due to the additional electrons in the system that occupy *nonbonding* states[53] which may prevent a closer metal-metal distance. The experimental values of the cohesive energies of the nitrides to which we can compare, in particular, for the 3*d* and 4*d* nitrides, exhibit a similar trend, but are about 6–18 % lower.[11,12] This overbinding is typical for DFT-LDA calculations.

It is interesting to note that the high binding energies, high melting points, and extreme hardness of these materials generally are typical of covalently bonded systems but that most of these refractory metal compounds exhibit metallic conductivities comparable to those of the pure transition metals. Their crystal (rocksalt) structure on the other hand is more typical for ionic crystals. In this respect, in the next section, we examine the electronic properties and the bonding nature.

B. Band structure

The DFT-LDA electronic bulk band structures are displayed in Fig. 2. It can be seen that all the materials are metallic in nature except for ScN, YN, and LaN, for which the band structure indicates that these materials are semimetals. For these systems the GGA is found to yield a very similar band structure to the LDA and thus brings about no improvement with respect to, for example, predicting semiconducting behavior as had been suggested by experiment. This is essentially the same result as has been found for the III-V nitrides,[35] where the GGA yields a very similar band gap as the LDA for AlN and GaN, while for InN the band gap remains negative.

Characteristic band separations are listed in Table II. $E_{\mathrm{Ns-N}p}$ is the energy gap between the N *s* band and the valence band complex, ΔE_d is the zone-center metal *d* band splitting, and $E_p - E_s$ is the N *p*–N *s* energy gap $E(\Gamma_{15}) - E(\Gamma_1)$. In each of the nitride groups, on going down the columns, the *d* band broadens and generally ΔE_d increases. From left to right across a row, a downward shift of the bands can be observed, in accordance with the sequential filling of the *d* bands—which is similar to what occurs in the bulk metals. As a consequence, we can observe the smooth trend of a decrease in $E_{\mathrm{Ns-N}p}$. Furthermore, ΔE_d exhibits a decrease from left to right (with the exception of LaN) and $E_p - E_s$ exhibits a smooth increase.

As Harrison and Straub[53] describe, ScN, YN, and LaN in the rocksalt structure, have eight valence electrons per atom pair, and only bonding states are filled. For TiN and VN, which have nine and ten valence electrons per atom pair, respectively, and similarly for ZrN, NbN (4*d*), and HfN, TaN (5*d*), the additional electrons occupy nonbonding states, which do not modify the bonding properties significantly, but do make the compound metallic. Only for transition metal nitrides further to the right in the periodic table do antibonding states become occupied—and these compounds are then

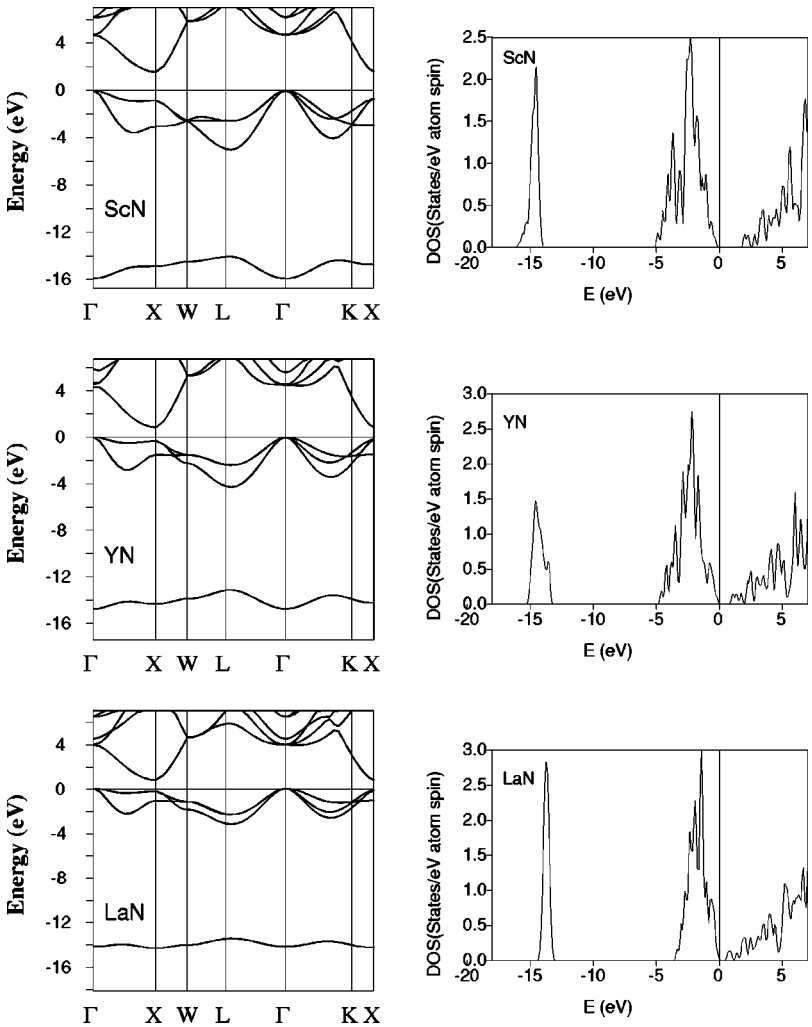

FIG. 3. Band structures (left panel) and density of states (DOS) (right panel) for ScN, YN, and LaN calculated using the screened-exchange LDA.

not stable in the rocksalt structure.[53] With respect to ScN (and YN and LaN), due to the complete filling of bonding states and the completely unoccupied nonbonding and antibonding states, ScN might indeed be inclined to be semiconducting.[22] As mentioned above, within the LDA and GGA we find ScN to be a semimetal (as for YN and LaN); as noted earlier, some experiments, however, have indicated that ScN may be a semiconductor. To investigate this possibility we performed calculations using the sX-LDA. We find that these materials are indeed semiconductors and with an indirect band gap: ScN has a band gap of 1.58 eV, YN 0.85 eV, and LaN 0.75 eV. The calculated band structures are shown in the left column of Fig. 3 and the total densities of states are shown in the right panel. The associated band separations are listed in parentheses in Table II. It can be seen that compared to the LDA band structure, in addition to the appearance of an indirect band gap, the N 2*s* bands lie 1.5–2.5 eV lower in energy.

We have learned very recently that two other theoretical investigations of the band structure of ScN have been reported, both of which also predict that it is a semiconductor: From local (spin) density calculations, including estimated quasiparticle corrections, Lambrecht[54] predicts an indirect band gap of 0.9 eV (significantly smaller than our value), and Gall *et al.*[55] using density-functional theory and the exact-exchange formalism predict an indirect band gap of 1.6 eV (in excellent agreement with our result); further, in this work[55] an experimental band gap of 1.3 ± 0.3 eV was determined from measurement of the optical properties—in particular, through transmission, reflection, and spectroscopic ellipsometry experiments, as well as by valence band photoelectron spectroscopy. The result provides confidence in our results also for YN and LaN, and so raises our expectation for early confirmation of our predictions for these materials.

C. Density of states

The total partial densities of states (DOS) for the nitride series studied are shown in Fig. 4 for the metal atom and for the nitrogen atom of the bulk compound, in addition to their state (s, p, d) resolved DOS's. These quantities indicate that there is a strong hybridization between the N states and the metal states with the energy position and shape of the partial DOS's for the N and metal atoms appearing very similar. The feature lying lowest in energy is the N 2*s* derived state. With respect to the valence band complex, there are two high density regions separated by a low electron density region. The bottom of the lower region involves metal s–N p states and above this, metal d (and some p)–N p bonding contributions.[8] The upper region, which, except for ScN,

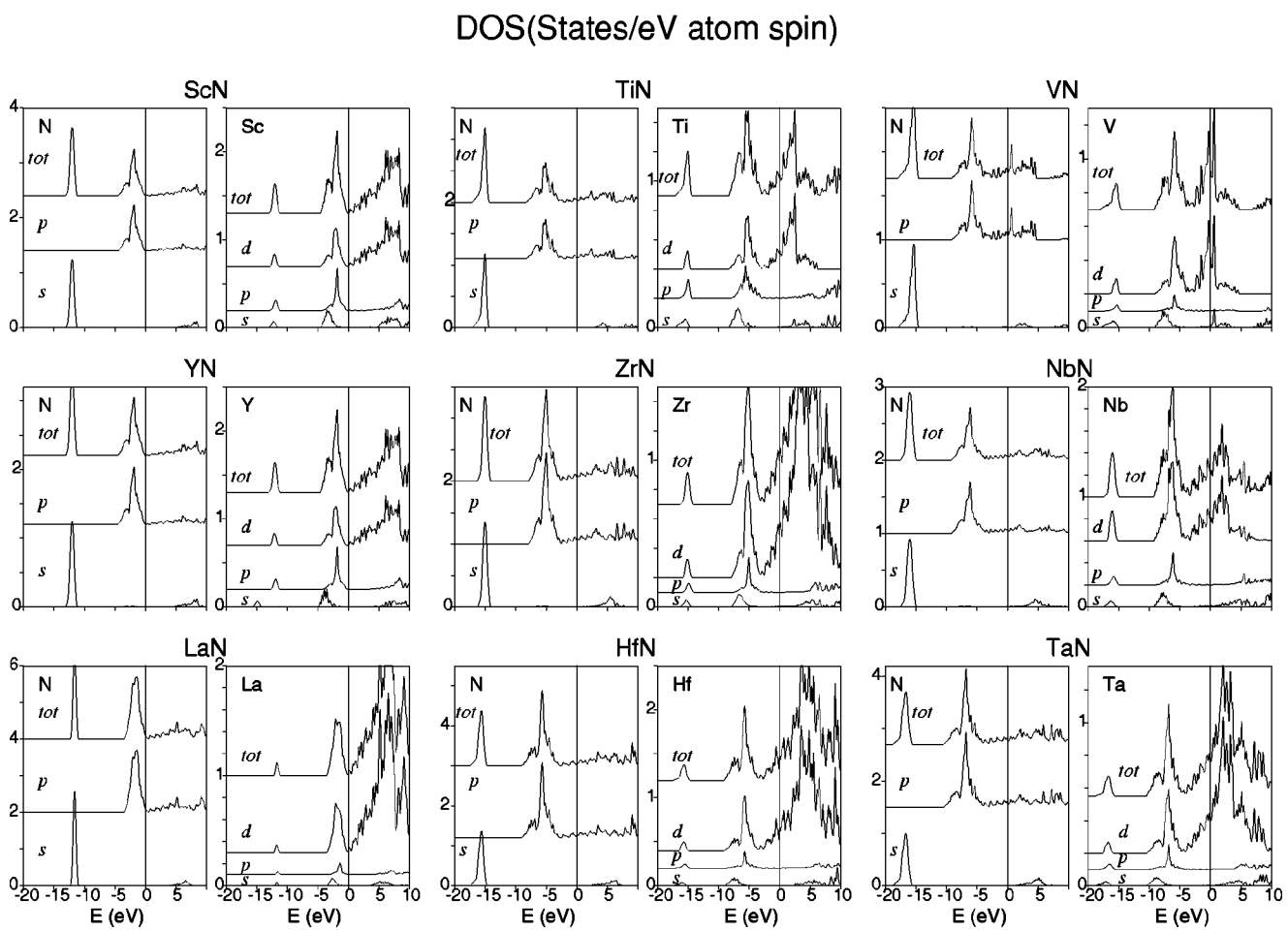

FIG. 4. Partial densities of states and their state resolved components for the early transition metal mononitrides studied, arranged corresponding to the position of the metal atom in the periodic table.

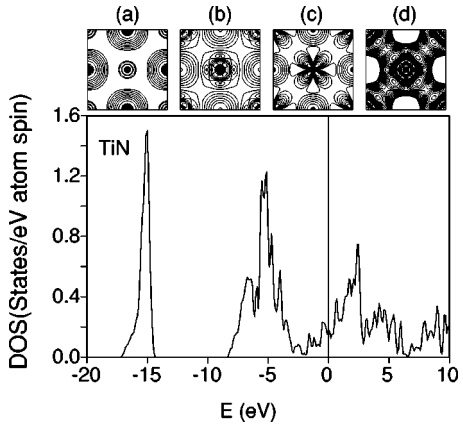

FIG. 5. Upper figures from left to right: Electron density distributions for TiN corresponding to the energy regions (a) -16 to -15, (b) -8 to -7, (c) -2 to -1, and (d) 5 to 6 eV with respect to the Fermi level. The N atoms are in the centers of the edges of the figures and the metal atoms are at the corners and center. The first contour line is at 0.001 e bohr^{-3} with a spacing of $\log_{10}$ 1.4.

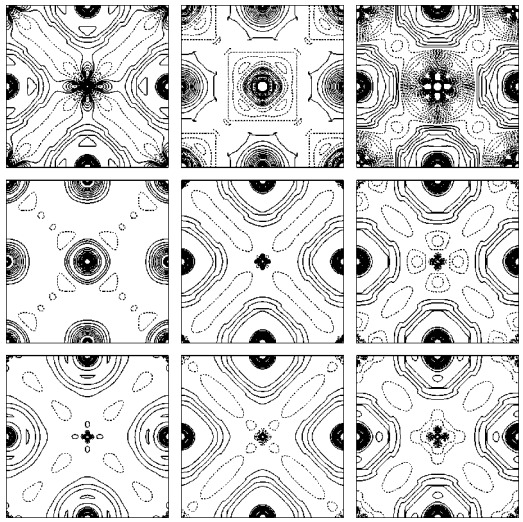

FIG. 6. Electron density differences $n^{\Delta}(\mathbf{r})$ (see text for a precise definition) between those of the bulk nitride material and those of the sums of their constituents, at the lattice constant of the bulk compound. The N atoms are in the centers of the edges of the figures and the metal atoms are at the corners and center. The first (negative) contour line is at -0.08 e bohr^{-3} with a spacing of 0.004.

YN, and LaN, is cut by E_F, is mainly due to metal *d* states with some N *p* component. Also the N *s* state mixes with the metal atom *s* states. These hybridizations are indicated from the decomposition of the partial DOS's into their *s*, *p*, and *d* contributions as seen in Fig. 4.

An indication of this bonding configuration can also be seen through plotting the electron density distributions in an appropriate narrow energy region. As an example, we show in Fig. 5, for TiN, the electron density distributions for states in the above-mentioned regions, namely, (a) -16 to -15 eV, (b) -8 to -7 eV, (c) -2 to -1 eV, and (d) 5 to 6 eV, with respect to E_F. The first energy range shows clearly that the states are predominantly N related with a small contribution from the metal. In the next region, at the bottom of the valence band, the states are composed of both N and metal orbitals, as are those in the next energy region. The unoccupied states at 5–6 eV are clearly essentially due to the metal atoms.

D. Difference charge densities

It has been proposed for such systems as those studied here, i.e., systems that involve the bonding of transition metals to nontransition metals, that the bonding can be thought of as consisting of two competitive processes:[50] (i) a loss in metal-metal bond strength due to the (usual) enlargement of the volume of the unit cell caused by the addition of N (or, e.g., O or C) in the interstitial positions of the fcc lattice, and (ii) an energy gain due to favorable bonding interactions with these metalloid atoms. With respect to this picture, as discussed above, we have investigated the energy cost to change the equilibrium volume of the metal to that of its nitride (but without N); the results were presented in Fig. 1(c) (lower curves). Not surprisingly, we found a larger energy cost for a larger volume expansion, i.e., for VN, NbN, and TaN. We also constructed the electron density redistribution due to the interaction of N and the metal atom, i.e., we calculated the difference in valence electron density,

$$n^{\Delta}(\mathbf{r}) = n_{NX}^{\text{bulk}}(\mathbf{r}) - n_{\text{N fcc}}(\mathbf{r}) - n_{X\ \text{fcc}}(\mathbf{r}), \tag{6}$$

where n_{NX}^{bulk}, $n_{\text{N fcc}}$, and $n_{X\ \text{fcc}}$ are the total electron densities of the bulk and the N and metal atoms at the (fcc) positions that they have in the nitride (*X*N) crystal. The results are presented in Fig. 6. It can be seen that for each material there is an increase in electron density at the N atoms and a decrease in the interstitial region between the metal atoms where the metal-metal bonding was formed in the reference structure. This charge rearrangement reflects the electronegative nature of N. For VN, ZrN, NbN, LaN, HfN, and TaN, there is also a decrease at the metal atoms, while for ScN, TiN, and YN, there is an increase in the electron charge density at the metal atoms.

These electron density rearrangements are reflected in the change in charge density contained in the muffin-tin and interstitial regions for the nitrides, as compared to the corresponding quantities in the separated, constituent systems where the atoms are at the (fcc) positions that they have in the nitride (*X*N) crystal. In all cases, the interstitial region was found to have lost charge density and the N muffin-tin sphere to have gained density. (For this analysis, for all systems, for consistency in the comparison, we used the same N muffin-tin radius of 1.5 a.u.) With the exception of LaN and HfN, the charge density in the muffin-tin sphere of the metal atom has also increased. We point out that to some degree this depends on the chosen metal muffin-tin radius (which is arbitrary); i.e., in some cases (VN, ZrN, NbN, TaN) the increase is just due to the tail of the electron density increase that is centered at the N atom which enters the metal muffin-tin sphere.

In view of the electronic properties investigated, we find that the bonding of these materials has a covalentlike character given the notable hybridization of N and metal states as found in the density of states; as seen from the above, however, there is also an ionic component with a significant charge transfer to the more electronegative nitrogen atom, as well as clearly a metallic nature (with the exception of ScN, YN, and LaN).

IV. CONCLUSION

Systematic full-potential linearized augmented plane wave calculations have been performed for a series of bulk early transition metal mononitrides. Equilibrium lattice constants and bulk moduli have been obtained as well as heats of formation and cohesive energies. Both the LDA and the GGA were employed and their performance compared. Both exchange-correlation functionals exhibit the same trends with the GGA yielding 1%–2% larger lattice constants, 10%–20% smaller bulk moduli, and 10%–30% smaller heats of formation compared to the LDA. With respect to available experimental results, the GGA yields lattice constants in overall closer agreement, but with a tendency to slightly overestimate them. The bonding nature of these materials can be described as covalentlike due to hybridization of N and metal states, but there is also some ionic character with electron transfer from the metal atoms to the nitrogen atoms, as well as the obvious metallic character. ScN, YN, and LaN are found from our sX-LDA calculations to be *semiconductors* with indirect band gaps of 1.58 eV, 0.85 eV, and 0.75 eV, respectively, in contrast to LDA and GGA results which predict that they are semimetals. Very recent unpublished experimental results[55] for ScN appear to verify this result and we hope future experiments can verify our predictions for YN and LaN as well.

ACKNOWLEDGMENTS

This work was supported by the National Science Foundation (through the Northwestern University Materials Research Center and the computing resources provided by the National Partnership for Advanced Computational Infrastructure at the San Diego Supercomputer Center). We thank Yip-wah Chung and Nate Newman for encouragement and discussions.

[1] H. F. George and H. K. John, Phys. Rev. **93**, 1004 (1954).
[2] A. Nigro, G. Nobile, V. Palmieri, G. Rubino, and R. Vaglio, Phys. Scr. **38**, 483 (1988).
[3] K. Kawaguchi and M. Sohma, Jpn. J. Appl. Phys., Part 2 **30**, L2088 (1991).
[4] K. Wakasugi, M. Tokunaga, T. Sumita, H. Kubota, M. Nagata, and Y. Honda, Physica B **239**, 29 (1997).
[5] S. Veprek, J. Vac. Sci. Technol. A **17**, 2401 (1999).
[6] U. Helmersson, S. Todorova, S. A. Barnett, J.-E. Sundgren, L. C. Markert, and J. E. Greene, J. Appl. Phys. **62**, 481 (1987).
[7] P. Nesládek and S. Veprek, Phys. Status Solidi A **177**, 53 (2000).
[8] D. A. Papaconstantopoulos, W. E. Pickett, B. M. Klein, and L. L. Boyer, Phys. Rev. B **31**, 752 (1985).
[9] V. P. Zhukov, V. A. Gubanov, O. Jepsen, N. E. Christensen, and O. K. Andersen, J. Phys. Chem. Solids **49**, 841 (1988).
[10] A. Fernández Guillermet and G. Grimvall, Phys. Rev. B **40**, 10 582 (1989).
[11] A. Fernández Guillermet, Phys. Rev. B **45**, 11 557 (1992).
[12] J. Häglund, G. Grimvall, T. Jarlborg, and A. Fernández Guillermet, Phys. Rev. B **43**, 14 400 (1991).
[13] H. Shimizu, M. Shirai, and N. Suzuki, J. Phys. Soc. Jpn. **66**, 3147 (1997).
[14] H. Shimizu, M. Shirai, and N. Suzuki, J. Phys. Soc. Jpn. **67**, 922 (1998).
[15] A. Filippetti and W. E. Pickett, Phys. Rev. B **59**, 8397 (1999).
[16] A. Filippetti, W. E. Pickett, and B. M. Klein, Phys. Rev. B **59**, 7043 (1999).
[17] P. J. Dismukes, M. W. Yim, and S. V. Ban, J. Cryst. Growth **13/14**, 365 (1972).
[18] T. D. Moustakas, R. J. Molnar, and J. P. Dismukes, Electro. Soc. Proc. **96**, 196 (1996).
[19] J. P. Dismukes and T. D. Moustakas, Electro. Soc. Proc. **96**, 110 (1996).
[20] D. Gall, I. Petrov, L. D. Madsen, J.-E. Sundgren, and J. E. Greene, J. Vac. Sci. Technol. A **16**, 2411 (1998).
[21] X. Bai, D. M. Hill, and M. E. Kordesch, in *Wide-bandgap Semiconductors for High-Power, High-Frequency, and High-Temperature Applications*, edited by S. Binari, A. Burk, M. Mellock, and C. Nguyen, MRS Symposia Proceedings No. 572 (Materials Research Society, Pittsburgh, 1999).
[22] G. Travaglini, F. Marabelli, R. Monnier, E. Kaldis, and P. Wachter, Phys. Rev. B **34**, 3876 (1986).
[23] R. Monnier, J. Rhyner, T. M. Rice, and D. D. Koelling, Phys. Rev. B **31**, 5554 (1985).
[24] W. Mannstadt, R. Asahi, and A. Freeman (unpublished).
[25] J. P. Perdew and M. Levy, Phys. Rev. Lett. **51**, 1884 (1983).
[26] L. J. Sham and M. Schlüter, Phys. Rev. Lett. **51**, 1888 (1983).
[27] R. W. Godby, M. Schlüter, and L. J. Sham, Phys. Rev. B **37**, 10 159 (1988).
[28] W. Kohn, A. D. Becke, and R. G. Parr, J. Chem. Phys. **100**, 12 974 (1996).
[29] M. Ernzerhof, J. P. Perdew, and K. Burke, in *Theory I Density Functional*, Vol. 180 of *Topics in Current Chemistry*, edited by R. F. Nalewajski (Springer-Verlag, 1996), p. 1.
[30] B. Hammer, M. Scheffler, K. W. Jacobsen, and J. K. Nørskov, Phys. Rev. Lett. **73**, 1400 (1994).
[31] B. Hammer, L. B. Hansen, and J. K. Nørskov, Phys. Rev. B **59**, 7413 (1999).
[32] L. Mitas and R. M. Martin, Phys. Rev. Lett. **72**, 2438 (1994).
[33] J. C. Grossman, L. Mitas, and K. Raghavachari, Phys. Rev. Lett. **75**, 3870 (1995).
[34] C. Fillipi, X. Gonze, and C. J. Umrigar, in *Recent Developments and Applications of Density Functional Theory*, edited by J. M. Seminario (Elsevier, Amsterdam, 1996).
[35] C. Stampfl and C. G. Van de Walle, Phys. Rev. B **59**, 5521 (1999), and references therein.
[36] P. Dufek, P. Blaha, V. Sliwko, and K. Schwarz, Phys. Rev. B **49**, 10 170 (1994).
[37] P. Dufek, P. Blaha, and K. Schwarz, Phys. Rev. B **50**, 7279 (1994).
[38] T. C. Leung, C. T. Chan, and B. N. Harmon, Phys. Rev. B **44**, 2923 (1991).
[39] B. M. Bylander and L. Kleinman, Phys. Rev. B **41**, 7868 (1990).
[40] A. Seidl, A. Görling, P. Vogel, J. A. Majewski, and M. Levy, Phys. Rev. B **53**, 3764 (1996).
[41] R. Asahi, W. Mannstadt, and A. J. Freeman, Phys. Rev. B **59**, 7486 (1999).
[42] R. Asahi, W. Mannstadt, and A. J. Freeman, Phys. Rev. B **62**, 2552 (2000).
[43] L. Hedin, Phys. Rev. **139**, A796 (1965).
[44] E. Wimmer, H. Krakauer, M. Weinert, and A. J. Freeman, Phys. Rev. B **24**, 864 (1981).
[45] L. Hedin and B. I. Lundqvist, J. Phys. C **4**, 2064 (1971).
[46] J. P. Perdew, J. A. Chevary, S. H. Vosko, K. A. Jackson, M. R. Pederson, D. J. Singh, and C. Fiolhais, Phys. Rev. B **46**, 6671 (1992).
[47] M. Fuchs, J. L. F. da Silva, C. Stampfl, J. Neugebauer, and M. Scheffler (unpublished).
[48] *Table of Interatomic Distances and Configuration in Molecules and Ions, Supplement 1956–1959*, edited by L. E. Sutton, Special Publication No. 18 (Chemical Society, London, 1965).
[49] V. Moruzzi, J. Janak, and A. Williams, *Calculated Electronic Properties of Metals* (Pergamon, New York, 1978).
[50] C. D. Gelatt,Jr., A. R. Williams, and V. L. Moruzzi, Phys. Rev. B **27**, 2005 (1983).
[51] F. R. de Boer, R. Boom, W. C. M. Mattens, A. R. Miedema, and A. K. Niessen, *Cohesion in Metals* (North-Holland, Amsterdam, 1988).
[52] W. T. Geng, Y. M. Zhou, and D. S. Wang, Chin. J. Comput. Phys. **16**, 372 (1999).
[53] W. A. Harrison and G. K. Straub, Phys. Rev. B **36**, 2695 (1987).
[54] W. R. L. Lambrecht, Phys. Rev. B **62**, 13 538 (2000).
[55] D. Gall, M. Städele, K. Järrendahl, I. Petrov, P. Desjardins, R. T. Haasch, T.-Y. Lee, and J. E. Greene (unpublished).
[56] H. J. Monkhorst and J. D. Pack, Phys. Rev. B **13**, 5188 (1976).
[57] W. Lengauer, J. Solid State Chem. **76**, 412 (1988).
[58] V. A. Gubanov, Z. W. Lu, B. M. Klein, and C. Y. Fong, Phys. Rev. B **53**, 4377 (1996).
[59] K. T. Park, K. Terakura, and N. Hamada, J. Phys. C **20**, 1241 (1984).
[60] M. van Schilfgaarde, A. Sher, and A.-B. Chen, J. Cryst. Growth **178**, 8 (1997).
[61] R. W. G. Wyckoff, *Crystal Structures*, 2nd ed. (Wiley, New York, 1963), Vol. 1, p. 86.
[62] A. N. Christiansen, Acta Chem. Scand., Ser. A **32**, 87 (1978).
[63] *Structure Reports*, edited by W. B. Pearson (International Union of Crystallography, Oosthoek, Scheltema, and Holkema, Utrecht, 1913–1993). TiN (Vol. 11, p. 170), VN (Vol. 8, p. 104),

YN (Vol. 21,p. 160), ZrN (Vol. 41A, p. 43), NbN (Vol. 30A, p. 155), LaN (Vol. 16, p. 105), HfN (Vol.17, p. 70), and TaN (Vol. 35A, p. 121).

[64] B. R. Zhao, L. Chen, and H. L. Luc, Phys. Rev. B **29**, 6198 (1984).

[65] P. Villars and L. D. Calvert, *Pearson's Handbook of Crystallographic Data for Intermetallic Phases* (American Society for Metals, Metals Park, Ohio, 1985).